Journal of Petroleum Exploration and Production Technology (2025) 15:47
https://doi.org/10.1007/s13202-025-01955-3

ORIGINAL PAPER - PRODUCTION ENGINEERING

# Synergistic application of Welan gum and polysaccharides for enhanced oil recovery

**Galymzhan Serikov[1] · Yermukhan Zhuniskenov[1] · Azza Hashim Abbas[2] · Peyman Pourafshary[1]**

Received: 26 July 2024 / Accepted: 9 February 2025 / Published online: 19 February 2025
© The Author(s) 2025

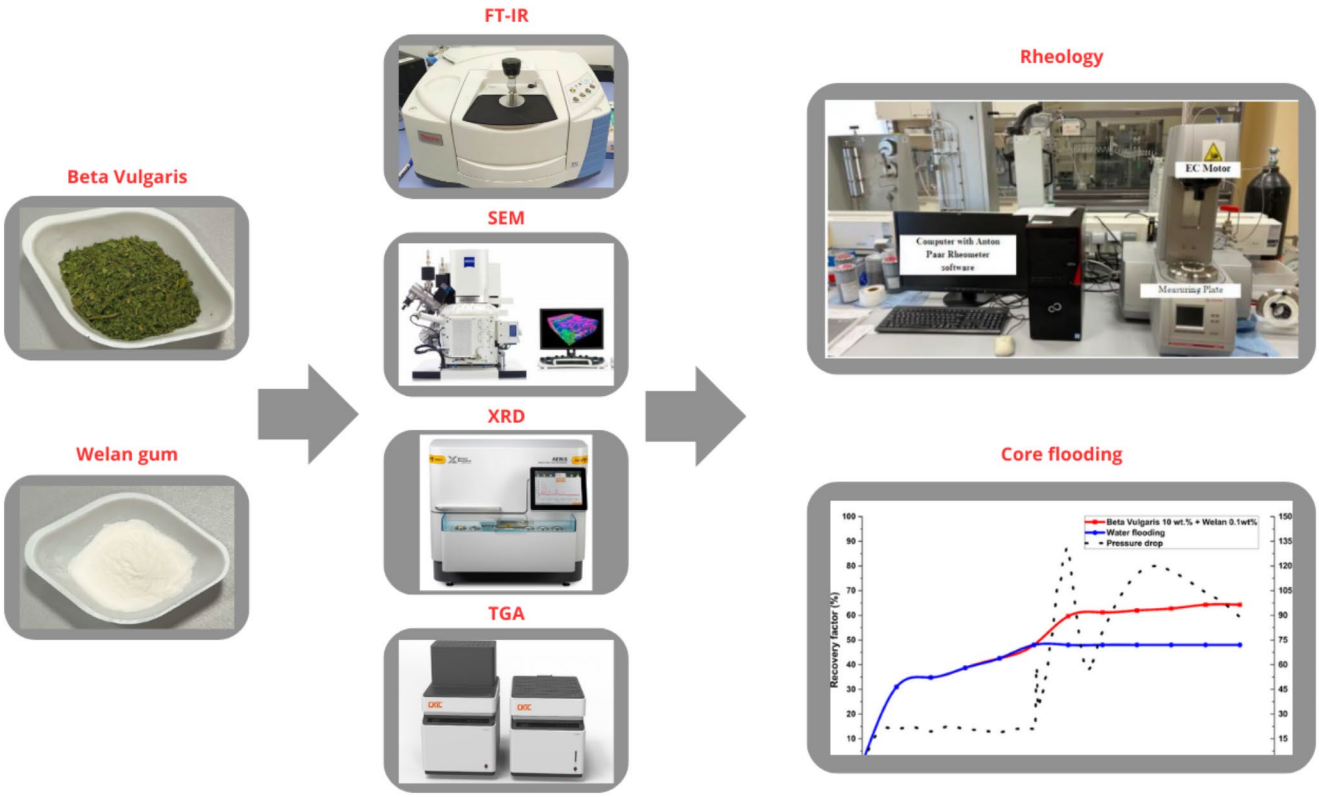
**Abstract** The use of natural polymers for Enhanced Oil Recovery (EOR) offers an eco-friendly alternative to synthetic polymers. This study introduces a novel approach by utilizing *Beta vulgaris* polymer and exploring its modification with Welan gum to enhance rheological performance. The polymers were characterized through SEM, FTIR, XRD, and TGA to assess their structural, thermal, and morphological properties. The study evaluates the effects of concentration, temperature, and salinity on rheological behavior along with core flooding. *Beta vulgaris* exhibited varying particle sizes with moderate viscosity (10 cP), which decreased by 80% at 55 °C in saline conditions, indicating poor thermal stability. Welan gum, with its rod-like structure, demonstrated superior thermal resistance. The composite blend of Beta vulgaris and Welan gum significantly improved viscosity (30 cP) and flow stability. All polymers followed the Ostwald–de Waele power law, with the composite blend enhancing the flow behavior index and stability by 75% and 10%, respectively. Core flooding experiments confirmed a 60% increase in oil fractional flow with natural polymers and 26% incremental oil recovery with a composite material injection. This study demonstrates the potential of combining *Beta vulgaris* and Welan gum as a sustainable, efficient solution for EOR, particularly in challenging reservoir conditions.

✉ Azza Hashim Abbas
azzahashim2008@gmail.com; ahh4000@hw.ac.uk

[1] Department of Petroleum Engineering, School of Mining and Geosciences, Nazarbayev University, Astana 010000, Kazakhstan

[2] Institue of Geoenergy Engineering, Heriot Watt University, Edinburgh EH14 4AS, UK

**Graphical abstract**




**Keywords** Flow behavior · Polysaccharides · Enhanced oil recovery · Welan Gum · *Beta vulgaris*

Abbreviations

| | |
|---|---|
| EOR | Enhanced oil recovery |
| FTIR | Fourier-transform infrared spectroscopy |
| HPAM | Hydrolized polyacrylamide |
| OOIP | Original oil in place |
| PV | Pore volume |
| SEM | Scanning electron microscopy |
| STA | Simultaneous thermal analyzer |
| TGA | Thermogravimetric analysis |
| XRD | X-Ray diffraction |

**Greek scripts**

| | |
|---|---|
| $c$ | Concentration (wt%) |
| $d$ | Diameter (cm) |
| $dP$ | Pressure drop (psi) |
| $k$ | Flow behavior index |
| $k_a$ | Absolute permeability (mD) |
| $k_o$ | Relative permeability of oil (mD) |
| $k_w$ | Relative permeability of water(mD) |
| $L$ | Length (cm) |
| ML | Molecular weight (g mole$^{-1}$) |
| $n$ | Consistency index |
| $P$ | Pressure (psi) |
| $R^2$ | Coefficient of determination |
| So | Oil saturation |
| Soi | Initial oil saturation |
| Sw | Water saturation |
| Swi | Initial water saturation |
| $T$ | Temperature (°C) |
| $\mu$ | Viscosity (cp) |
| $w$ | Weight (g) |
| $\varphi$ | Porosity |
| $\gamma$ | Shear rate (s$^{-1}$) |

## Introduction

Polymer flooding is recognized as one of the most efficient EOR methods in the moderate reservoir conditions. Injection of polymers underground increases oil production by pushing oil with high viscosity fluid. The major mechanisms of polymer flooding are the decrease of mobility ratio by viscosifying injected water and consequently reduction of fingering in the reservoir (Gbadamosi et al. 2022a) and viscoelastic behavior (Pal et al. 2016). The first application of polymers in EOR was at Daqing field in China, where

oil recovery was uncreased by 12% of OOIP since 1996. Injected polymer viscosity enabled piston like movement in the reservoir and consequently higher oil recovery. The major parameter of polymer selection is the rheological property and structural differences. Detailed analysis of polymer structure and functional groups along with viscosity measurements is the key factor of polymer assessment (Wever et al. 2011). Recent study has shown that most polymers tend to lose rheological properties at harsh reservoir conditions of high temperature and salinity. According to Jouenne (2020), elevated temperatures and salinity negatively affect polymer performance, however the combined effect of temperature and salinity facilitates the viscosity drop. Results of viscosity measurements confirmed low tolerance of hydrolyzed Polyacrylamide (HPAM) to harsh conditions. Sun et al. (2022) suggested the application of supramolecular polymers as the temperature and salinity resistant alternatives to existing natural and synthetic polymers. The main difference of supramolecular polymers is the presence of non-covalent interactions which easily adapt for the harsh reservoir conditions and are tolerant to elevated temperatures. The review of biopolymer application has shown that natural polymers also have a moderate resistance to harsh reservoir conditions (Pu et al. 2018). Analysis of the rheological properties of natural polymers and composites is an issue of utmost importance (Druetta et al. 2019; Bai et al. 2015; Needham and Doe 1987; Abbas et al. 2024; Zhao et al. 2024).

One of the most effective synthetic polymers used in EOR is HPAM. In the study, HPAM and biopolymer Xanthan have been adopted in polymer flooding projects at Daqing field's Mesozoic Cretaceous sandstone reservoir. Early field pilots with modified Xanthan gum at Yumen oil field in China showed promising results, but HPAM was favored due to lower cost and better stability under reservoir conditions (Han et al. 1999; Ezeh et al. 2021). Most EOR field projects rejected natural polymers due to their high costs and low stability under bacterial attacks. The effectiveness of the polymer at these conditions is improved with the addition of surfactants, nanoparticles or composite polymers. The application of hydrophobically modified HPAM in high salinity environment have shown that additional co-polymer groups shield the polymer, thus preventing it from coiling and lose of viscosity (Bhut et al. 2019). Other studies considered the polymer and nanoparticle emulsions. Results of Pal et al. (2019) illustrate that oil movement is facilitated in the presence of silica nanoparticles and addition of polymers could increase the oil recovery. Druetta et al. (2019) conducted the analysis study on the simulation with the effect of nanoparticles on the polymer performance. Although these methods are quite promising, natural polymer could have the same effects on the oil extraction and are more stringent environmental regulations.

Natural polymer has proved to be highly resistant to elevated temperatures and salinity. Studies by Agi et al. (2018) shows that in some cases the effectiveness of natural polymers outperform the synthetic. Gbadamosi et al. (2022b) studied the effectiveness of Okra polymer as an EOR agent at a seawater salinity and 80 °C temperature. Results of core flooding showed additional 12.7% of oil recovery.

(Ojo Oladimeji et al. 2013) studied okra and discovered that the optimum oil recovery was achieved when the polymer viscosity reached 2.6 cP, while a further increase in viscosity did not yield significant improvement in oil recovery. Agi et al. (2019) showed that application of okra as a biopolymer resulted in 13% additional recovery with Sarawak crude oil (Agi et al. 2019). The study conducted by Abbas et al. (2022) showed that okra yielded additional recovery of 7% for a heavy oil from Kazakhstan field (Abbas et al. 2022). Zamani et al. (2023) used Tragacanth gum extracted from the Astragalus plant as a natural polymer in chemical EOR experiments and produced 7–9% of additional recovery (Zamani et al. 2023). Gao (2016) demonstrated that welan gum, an anionic polysaccharide, recovered 70% OOIP, while further injection did not yield additional recovery, showing its limited capability to reduce residual oil saturation (Gao 2016). Guar gum demonstrated the ability to produce 16% incremental oil recovery (Musa et al. 2021). Chia seeds, a water-soluble anionic heteropolysaccharide, resulted in 16–21% recovery in sandstone experiments (Nowrouzi et al. 2023).

Soluble carbohydrate polymers are water-soluble macromolecules that consist of long chains of sugar units. Their solubility depends on the linkage and branching of the sugar units. These carbohydrates range from simple sugars to complex oligosaccharides and polysaccharides. For example, the Swiss chard in the wild (*Beta vulgaris* L. var. cicla) is a source of food in North Africa. During the cooking process, the *Beta vulgaris* leaves display a viscous behavior. A previous study on *Beta vulgaris* displayed phytochemical screening, which showed that these fatty acids are present (stearic, palmitic, linoleic oleic, and linolenic acids), phospholipids, glycolipids, polysaccharides, ascorbic acid, folic acid, pectins, saponins, flavonoids (apigenin), phenolic acids, and betalains (Mzoughi et al. 2019; Gao et al. 2009). Another study reported compositional variation with chemicals such as moisture, fat, carbohydrates, protein, ash, and crude fiber for non-green leaves (Kale et al. 2018). The combination of soluble carbohydrates and the complex nature of the leaves can be presented as polymeric fluids. In addition, *Beta vulgaris* contains saponin that can reduce the IFT (Adenutsi et al. 2023; Brezhneva et al. 2001).

Another aspect to consider in the characterization of polmyers is the adsobsion of polymers on the rock surfaces. Polymer adsorbtion basicly decreases the efficiency of the injected polymer as some part of it remains on the rock surface leading to decrease in concentration and efficiency. The basic mechanism of polymer adsorbtion is the polymer molecule interaction with the rock surface. This happens because of electromagnetic forces of charched polymers and charges on the rock surface due mineral presence (Agi et al. 2018). Several studies on adsorption of polymers have shown similar behavior on sandstones. According to Li et al. (2017), KYPAM (commercial Chinese polymer based on polyacrylamide) adsorption on a sandstone surface varied from 22.53 to 49.58 μg $g^{-1}$, resulting in decrease in polymer performance. Moreover, it was revealed that polymer adsorption was significantly increased with the increase in polymer concentration, higher molecular weight, and soaking time. Analysis of core has shown that polymer retention led to mechanical entrapment and decrease of permeability in the core. The study conducted by Fu et al. (2021) evaluated the performance of Welan gum adsorption on sandstone (mainly quartz). Results of adsorption experiments indicated that 0.5 mg $g^{-1}$ of Welan was adsorbed at the lowest polymer concentration of 500 ppm. Comparing the results of synthetic and natural polymers, it is clear that Welan gum has a tendency to adsorb more on a rock surface. However, for this new composite material study the effect of Welan gum adsorption along with *Beta vulgaris* was not studied.

This work aims to explore natural polymer sources such as wild *Beta vulgaris* for enhanced oil recovery, which was never discussed in petroleum engineering and remains under-evaluated. The study offers new physiochemical properties by evaluating the synergy of *Beta vulgaris* polymer and Welan gum-successful natural polymers. The experiments span between polymer characterization and petroleum examinations. The examination includes the effects of concentration, temperature, and salinity on polymer's rheological properties. This study represents a significant advancement in the utilization of natural polymers for offshore field application.

## Methodology

The rheological characteristics of polymer solutions have risen in the context of porous media. Therefore, the proposed methodology dissects the natural polymer *Beta vulgaris* performance and its mixture with Welan gum for EOR.

### Materials

*Beta vulgaris* was sourced from Riyadh, Kingdom of Saudi Arabia (KSA). They were sun-dried for three days, pulverized, and stored at − 10 °C. Welan gum was produced by Shanghai Yizong Biotechnology company and delivered from China (99% purity). The sodium chloride provided by Sigma Aldrich (MW 58.44 g $mol^{-1}$, 99% purity) was used in this study. The oil, dodecane, used in this study is synthetic and provided by Sigma-Aldrich. Dodecane has 98% purity and a molecular weight of 170.34 g $mole^{-1}$. The oil viscosity and density were 1.34 cP and 0.746 g $cm^{-3}$, respectively. The core used is Indiana Limestone. This core was supplied by Kocurek Industries from the USA.

### Polymer preparation

200 g of the dried *Beta vulgaris* leaves were mixed in 1000 ml of deionized water (DIW). The mixture was heated at 73 °C temperature for 30 min. The solution was left to cool down before centrifuging. The centrifuging device that were used was the Biosan laboratory refrigerated centrifuge LMC-4200R. The solution sample was distributed into 50 mL lab bottles to be suitable for centrifuging devices and placed inside. Samples were left for 10 min under 4200 rpm.

A series of polymer stock solutions were prepared at varying concentrations of 5, 10, and 15 wt% for a preliminary investigation. The investigation was designed to identify the optimal concentration. Subsequent experiments aimed to examine and select Welan gum concentrations. Welan gum studied at 0.05, 0.1, and 0.2 wt% concentration. The economic industrial limit in oil and gas practice governed the targeted concentration.

The composite material preparation study was conducted with the mixing of *Beta vulgaris* polymer at the optimum concentration of 10 wt%, as being the most efficient and stable, with Welan gum at concentrations of 0.05, 0.1, and 0.2 wt%. Polymer solutions were initial mixed in a ratio of 1:1 for a consistent study. Results of initial mixing samples of 10wt% of *Beta vulgaris* with 0.05 wt% showed minor improvement in viscosity after mixing 1:1. In the case of Welan gum concentration increase to 0.2 wt% the effect of *Beta vulgaris* as a natural additive polymer was diminished by full domination of Welan gum in the solution. After this sensitivity analysis mixing of 10 wt% of *Beta vulgaris* with 0.1 wt% of Welan gum was suggested at a ratio of 1:1 to achieve stable and efficient polymer composite material with a viscosity of around 20 cp.

## Chemical characterization

Fourier transform infrared (FTIR) spectroscopy is a tool to determine and characterize the functional groups of targeted composition. This analytical method is generally used in the determination of organic, polymeric, and inorganic compounds. In this study, a Nicolet iS10 FTIR spectrometer was utilized to receive FTIR spectra. A tool has a ZnSe flat crystal. The FTIR spectra were identified through OMNIC software. A scanning electron microscope (SEM) is a high-resolution microscope used to see detailed pictures of the sample structure. A detailed image of the sample was taken by adjusting the needed resolution and position. SEM used in this study is the Zeiss Crossbeam 540 by Zeiss Group from Jena, Germany. X-ray Diffraction (XRD) -Powder XRD equipment (Rigaku, Japan)-is a pivotal technique in polymer characterization, offering insights into crystalline structure, phase identification, and degree of crystallinity.

Thermogravimetric analysis (TGA) is an important part of polymer characterization and its thermal stability. TGA analyzes the mass loss with the increase in temperature, which is an indicator of compositional and structural changes. Results of TGA usually aid in evaluating polymer stability under high temperatures and decomposition points. In this wort, in a nitrogen atmosphere, TGA of *Beta vulgaris* and Welan gum samples was performed using a Simultaneous Thermal Analyzer (STA) 6000 with heating rate 10 °C $min^{-1}$.

## Rheology test

As the viscosity of the polymer plays a pivotal role in the EOR, the rheology test was conducted on polymers to ensure their suitability under reservoir salinity and temperature. Physica MCR-302 and Austrian Anton Paar rheometer were used to conduct the rheology tests. Basic settings for measurements are as follows: shear rate values from 1 to 1000 1 $s^{-1}$, and viscosity was measured at different temperatures in the range of 25–55 °C with 10 °C increments for all concentrations.

## Oil displacement study

The porosity of the core was measured using the HEP-P Helium porositimeter by Vinci Technologies. After measurement of the core for three times averaged porosity from helium injection estimated as 18.5%. The displacement experiment aimed to evaluate the polymer's effectiveness and was carried out using the ACA-700 apparatus, also provided by Vinci Technologies, as illustrated in Fig. 1. The

Made with VisualParadigm For non-commercial use

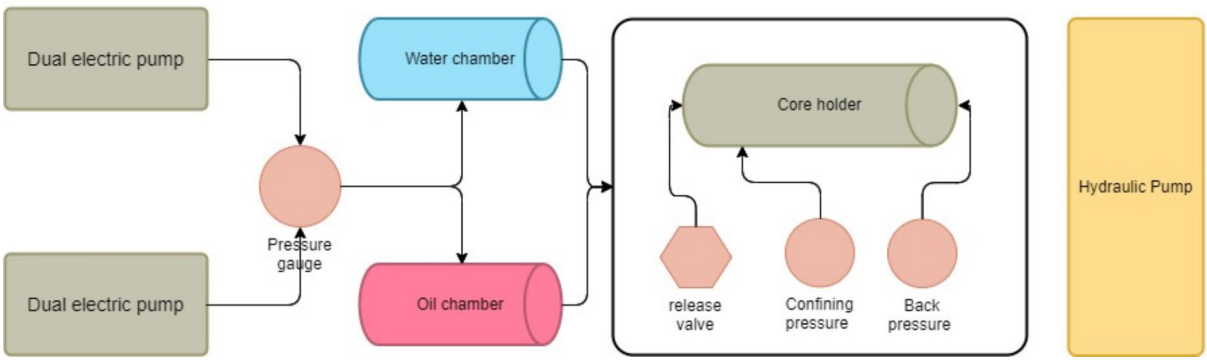



**Fig. 1** Core Flooding flow chart diagram

apparatus has two fluid holder chambers, one for injection fluid and one for water. The mechanism of the core flooding system works through pumping deionized water to regulate the injection flow rate. The pressure was monitored using two pressure gauges. The core used in this flooding is Indiana Limestone, a carbonate core similar to Kazakhstan reservoir rocks. Dimensions and weight of the cylindrical core were measured before core flooding. The core length was measured at 7.62 cm, and the diameter was measured at 3.81 cm. The characteristics of the core are presented in Table 1. Initial core preparation:

- Immertion of the dry core into oil bath for 24 h to reach oil-wet system.
- Oil is injected into a saturated core from oil bath and permeability values are measured.
- Saline water is injected into a core fully saturated with oil at rates from 1 to 5 cc $min^{-1}$.
- Oil was injected into a core saturated with saline water and oil.
- During all stages of core preparation pressure drop across the core was recorded to calculate permeability. Permeability was calculated using Darcy's Law.

Core flooding system preparation consists of setting confining pressure and back pressure of 1100 and 400 psi, respectively. The ambient temperature was constant in all experiments, which is 25 °C. During the pre-flush stage, 3 pore volumes (PV) of brine were flooded through the core. The size of the injection for the main flush stage was determined based on observations of oil cut, involving a 1 PV injection of polymer solution at a rate of 1 cc $min^{-1}$. The final stage consisted of an additional 3 PV of brine flooding.

## Result and discussion

### Polymer characterization

#### SEM analysis

The SEM was used to observe the polymer structure under the microscope. Figure 2a shows *Beta vulgaris* varying in size and non-uniform distribution in both solid and liquid. The morphology suggests irregular shapes with some aggregation. Hence, the structure is complex and not consistent in the solution. The surface texture appears relatively rough and porous, which could imply a high surface area. In previous studies, the polysaccharide from natural material showed features of a reticular layer characterized by uniformly sized and distributed channels or exhibited a compact structure with a smooth surface and flocculent fibers by different drying methods. The observation of *Beta vulgaris* is aligned with the layered observations (Kong et al. 2015). The SEM image of Welan gum in Fig. 2b shows the varied particle sizes, but the components seem more uniform than those of a more controlled synthesis or processing method. The image exhibits rough surface with large, irregular particles. Some pores and cracks are visible, suggesting a brittle nature. The solid Welan gum structure shows smoother regions with large pores. The circular features may be indicative of entrapped air or other materials within the gum structure that was not observed for *Beta vulgaris*. Overall image appears less rough and more compact than Fig. 2a, with fewer visible pores. Previous studies have shown that the surface of the welan gum displays a compact texture. This indicates intermolecular interactions promoted within the polysaccharides and contributed to the hydrogel network (Zhao et al. 2022).

In the discussion of blending polymers, it is crucial to examine the morphology of the blend. The two natural polymers must be workable under high salinity; thus, it is necessary to determine whether the sample differs from the origins of both components. The dried sample of the solution confirms that the newly generated structure does not resemble either *Beta vulgaris* or Welan gum.

The major difference, as seen in Fig. 2c, is that the surface is not flat, likely due to the encapsulation of salt crystals. The edges appear smoother. The SEM of the combined material reveals defined, well-edged nanoscale that provides an early indication of enhanced adhesion between different phases, improving the overall mechanical properties of the polymer blends(Khan et al. 2019). The origin source of polysaccharide can result in major differences. For instance Welan gum is a microbial polysaccharide while *Beta vulgaris* is plant source.

#### FTIR analysis

The results of FTIR are presented in Fig. 3 and supported by the findings in Table 2. According to the FTIR analysis shown in Fig. 3, the broad and intense peak at approximately 3294 $cm^{-1}$ for Welan gum is associated with the hydroxyl groups within the sugar ring, which experiences vibrational stretching. Additionally, two distinct peaks in the range

**Table 1** Core characteristics

| Diameter, cm | Length, cm | Dry weight, g | Wet weight, g | Pore volume, cc | Porosity | Absolute permeability, mD | Effective permeability, mD | Soi | Swi |
|---|---|---|---|---|---|---|---|---|---|
| 3.81 | 7.62 | 176.83 | 188.92 | 17 | 0.185 | 137.7 | 26.7 | 0.742 | 0.258 |

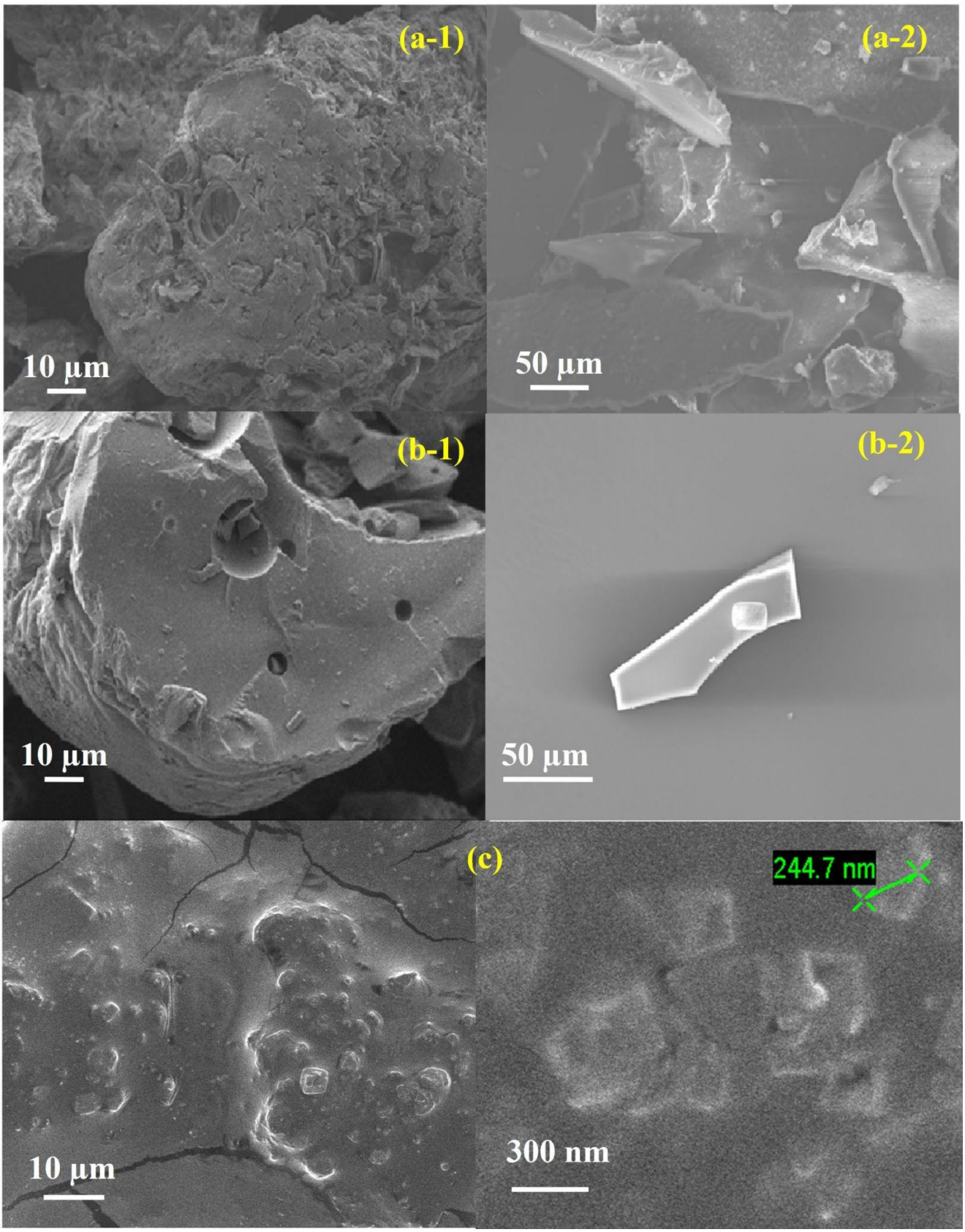



**Fig. 2** **a** SEM image of *Beta vulgaris* 1 solid and 2 in solution, **b** SEM image of Welan gum 1 solid and 2 in solution, **c** solution of *Beta vulgaris*/Welan in saline condition

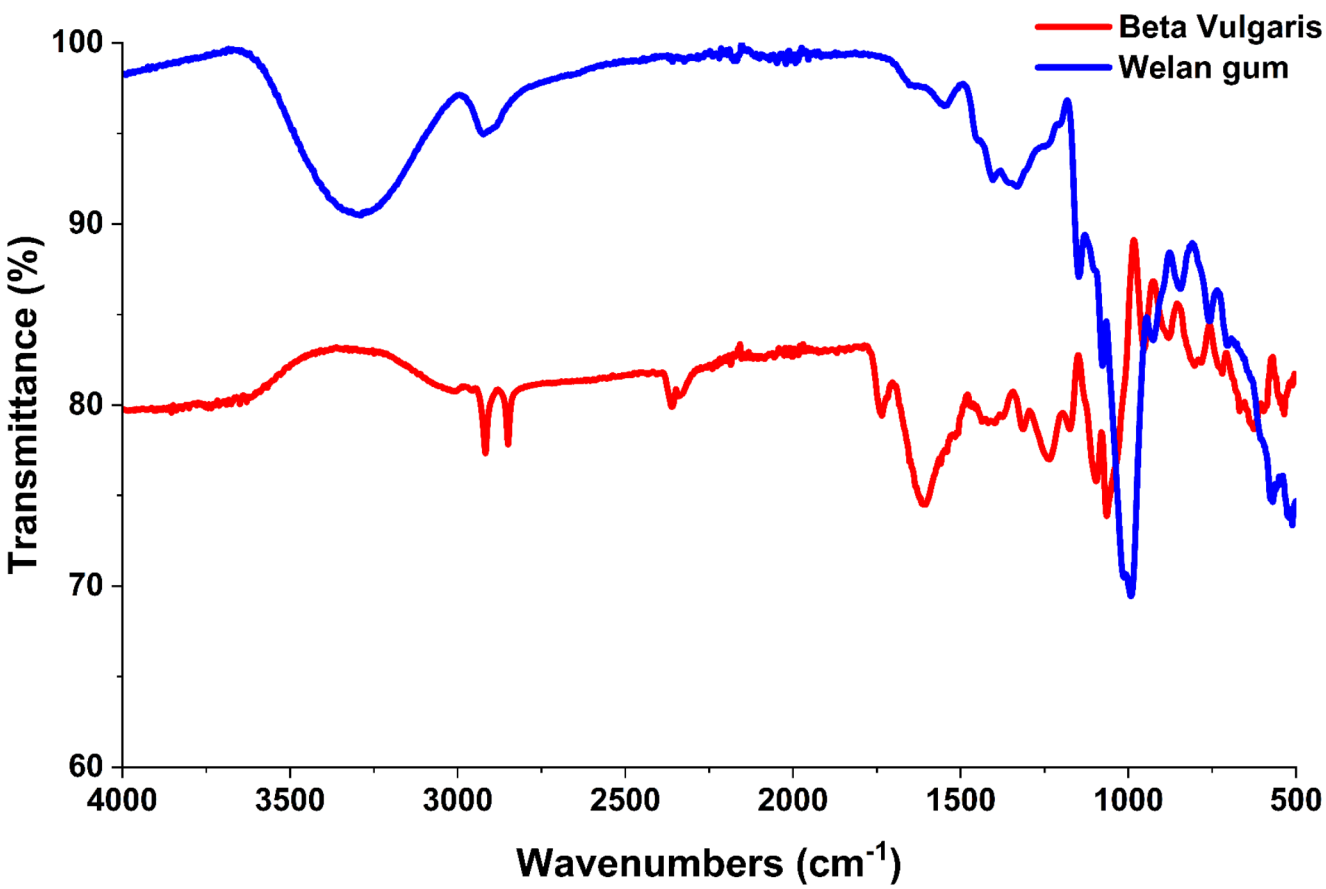



**Fig. 3** FTIR of *Beta vulgaris* and Welan gum

between 2926 $cm^{-1}$ and 1409 $cm^{-1}$ were identified as characteristic of polysaccharides. The presence of pyranose units in the polysaccharide molecule is related to glycosidic and hydroxilic bonds, as indicated by peaks in the 1000–1200 $cm^{-1}$ range (Cai et al. 2024). In the anomeric region (950–700 $cm^{-1}$), a distinctive absorption peak at 925 $cm^{-1}$ was observed, indicating the functionality of mannose.

FTIR results of *Beta vulgaris* depicted in Fig. 3 showed the same hydroxyl group peak at 3200 $cm^{-1}$ as Welan gum, showing polysaccharide functional groups with stretching. The distinction from synthetic polymers is noticed with the lack of narrow amide, amine groups peaks in the range of 3300 $cm^{-1}$, and 3100 $cm^{-1,}$ respectively. Double peaks at the wavelength of 2916 $cm^{-1}$ and 1849 $cm^{-1}$could be attributed to the C–H group signal, which experiences stretching and bending in the saturated $CH_2$ groups, eliminating the possibility of double, triple bonds and aromatic groups. A distinctive peak at 1610 $cm^{-1}$ could be related to the carboxyl group presence (RC=OR), which was not observed for Welan gum. This group leaves possibilities for ester, ether and organic acid groups. Moreover, ether (C–O–C) groups at the wavelength of 1235 $cm^{-1}$ were also noticed in the fingerprint region range. Overall, the FTIR analysis of Welan gum and *Beta vulgaris* showed the same functional groups of natural polysaccharides with cyclic rings of sugar family alcohols. From the chemistry side of view, the broader and more uniform hydroxyl peaks observed in Welan gum suggest stronger and more extensive hydrogen bonding networks, which are crucial for higher viscosity. This supports the hypothesis that welan gum can enhance the composites' viscosity. For *Beta vulgaris*, the Carboxyl groups are linked with components in fatty acids and amino acids. These molecules can interact with the naphthenic group in oil, producing soap-like material. Moreover, it allows further adsorption to the rock if the quantity of metals is high(Klecker and Nair 2017; Quiroga-Becerra et al. 2012). Lastly, although FTIR provides information about the functional groups present in a material, it could also be used to analyze the crystalline structure. General indicator of the crystalline structure is the presence of sharp peaks and broad for the amorphous materials. Results of FTIR testing show that for both polymers the peaks are broad corresponding to amorphous structure of materials, however additional XRD is nessesary to confirm the observation.

**Table 2** Functional group identification summary

| Functional group | Compound (functional group) | *Beta vulgaris* | Welan gum |
|---|---|---|---|
| Hydroxyl group | –OH | Peak at 3200 $cm^{-1}$ | Broad peak around 3294 $cm^{-1}$ |
| Amide and Amine groups | –NH2,–CONH2 | Absence of narrow peaks typically found in 3300–3100 $cm^{-1}$ range | N/A |
| C–H groups | –CH2– | Double peak at 2916 $cm^{-1}$ and 1849 $cm^{-1}$ | Two distinct peaks observed between 2926 $cm^{-1}$ and 1409 $cm^{-1}$ |
| Carboxyl groups | –COOH | Peak at 1610 $cm^{-1}$ | N/A |
| Ester, ether, and organic acid groups | –COOR,–O–,–COOH | Possible presence due to carboxyl group peak at 1610 $cm^{-1}$ | N/A |
| Ketone and aldehyde groups | > C = O | Absence inferred from (C–O) group stretching at 1065 $cm^{-1}$ and lack of free hydrogen vibration | N/A |
| Ether (C–O–C) groups | –O– | Identified at 1235 $cm^{-1}$ | Similar structures within polysaccharides |
| Protein content | –NH2 (in amino acids) | Traces at 1541 $cm^{-1}$ | N/A |
| Pyranose units | –O– (in sugar rings) | N/A | Evidenced by peaks in the 1000–1200 $cm^{-1}$ range |
| Mannose functionality | –O– (in mannose units) | N/A | Specific absorption peak at 925 $cm^{-1}$ within the anomeric region (950–700 $cm^{-1}$) |

### XRF analysis

Observing the result in Fig. 4 shows a basic indication of the crystallinity of both polymers. However, Welan gum may have larger or more well-defined crystalline regions than *Beta vulgaris*. *Beta vulgaris* has multiple sharp peaks throughout the 2θ range of 15°–30°, suggesting various planes of crystalline structure. *Beta vulgaris* XRD pattern reveals narrow, sharp peaks that indicate the formation of the crystal structure, as shown in Fig. 4. As a result, it was assumed that *Beta vulgaris* has high crystallinity powder. It is worth noting that the high-intensity peaks also refer to metallic impurities in the sample. As for Welan has displayed a more amorphous structure in comparison because of a few small visible crystalline peaks. The amorphous nature of the polymer is also shown by a broad peak between 10 and 30 degrees. The existence of tiny peaks indicates the presence of other elements.

### TGA analysis

The results of TGA are presented in Fig. 5. The general trend for both lines in Fig. 5 is the same, stating that both polymers have a similar thermal resistance. Noticeable mass reduction is noticed at a higher temperature of 200 °C for both Welan gum and *Beta vulgaris*. From the detailed analysis of welan gum, weight loss is significant between the 30–500 °C. At 500 °C, the weight loss reaches to 68%. Further, polymer carbonization occurs from 500 °C to 800 °C, and the converted product mass is 32%. Similarly, *Beta vulgaris* exhibits a weight loss profile parallel to Welan gum but decomposes more rapidly. At 500 °C, a weight loss of 62% was achieved while the residue was approximately 9% at 800 °C.

Statistically, the difference of 6% at 500 °C suggests that Welan gum maintains a better structure than *Beta vulgaris*. It is well known that the *Beta vulgaris* decay corresponds to polysaccharide conversion, and the difference results from polysaccharide sources and molecular weight. The *Beta vulgaris* begins to decompose rapidly at 200 °C, aligning with the loss of functional groups like carboxyls and less stable ethers, whose presence is confirmed by the FTIR.

The mass loss for both polymers at this temperature is less than 5%. This indicates that increased temperature conditions will not significantly affect their rheological properties. Generally, the results support the stability and functionality of polysaccharide polymers and endorse them for moderate temperature for the EOR.

## Optimum concentration selection

Previous research indicates that polymer viscosity increases with concentration, but excessive amounts may clog pores, restricting oil flow. Maximum effective concentrations are typically low. 0.3 wt% is often cited as the upper limit (Pramadika et al. 2019), while 0.05 wt% is the lowest effective biopolymer concentration (Ferreira and Moreno 2020).

The results in Fig. 6 show that increasing the concentration corresponded with the viscosity improvement. However, the selection of *Beta vulgaris* is conditioned by the highest possible effective concentration and controlled by

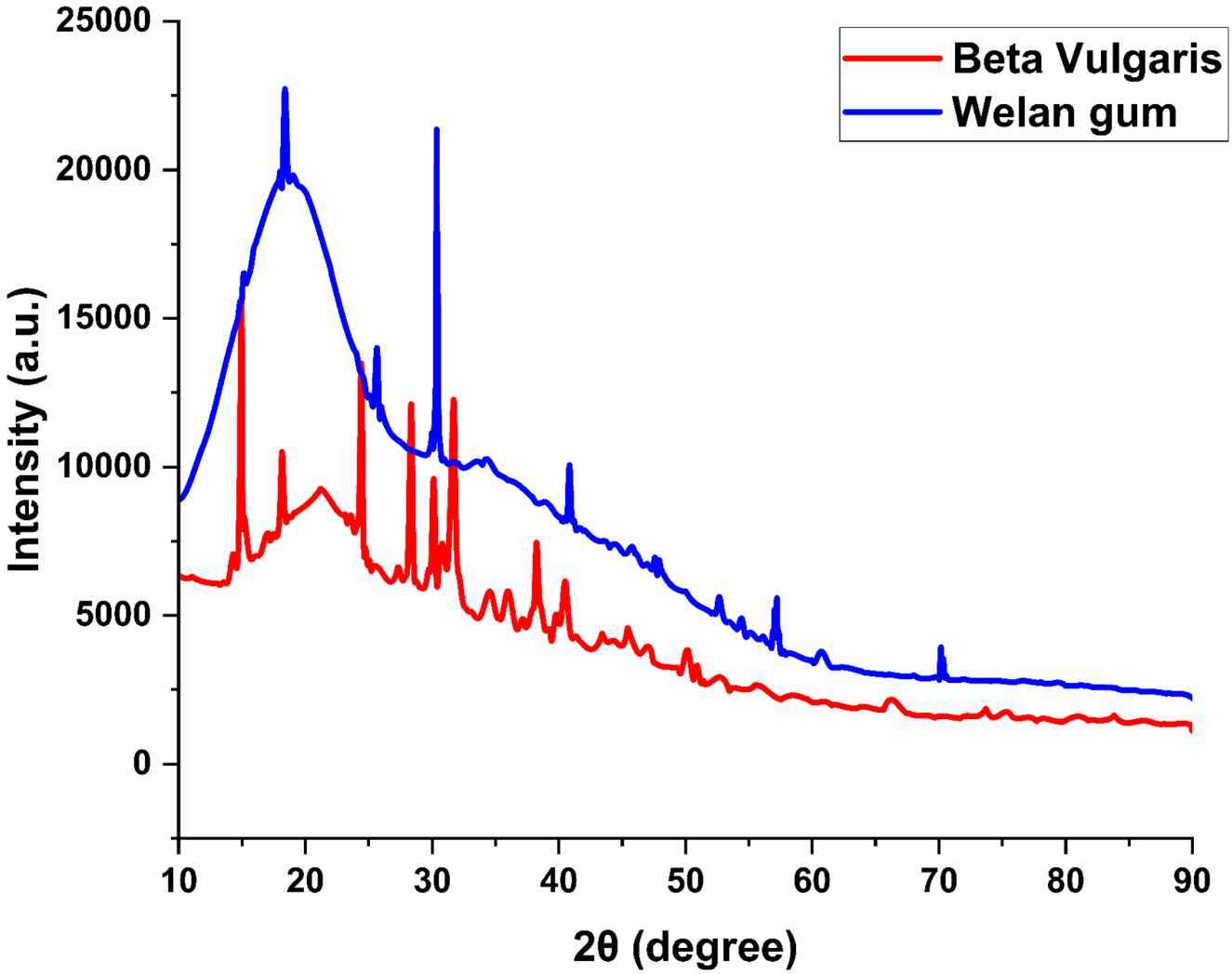



**Fig. 4** XRD images of *Beta vulgaris* and Welan gum

the economic limit. Thus, 10 wt% represents the highest effective concentration, which remains economically viable.

The observation on welan gum notably shows that viscosity is directly proportional to polymer concentration. Doubling the concentration of polymers leads to a corresponding doubling of viscosity. This is because as more polymer chains increase molecular drag and interaction forces. Thus, a Welan gum concentration of 0.1 wt% is appropriate for polymer flooding operations because of its cost-effectiveness and viscosity values comparable to *Beta vulgaris*. Additionally, to ensure an accurate composite/blend effect estimation by choosing similar viscosity attributes, resulting in the best compatibility expectancy(Fredi and Dorigato 2023).

The obtained rheological in Fig. 6 study have established that any increasing of concentration give more viscosity under the reservoir condition. However, by thorough analysis it shows that between the two polymers the relationship is not following similar proportional. This links the previous sensitivity analyses that supported a direct proportionality between polymer concentration and viscosity, as evidenced by a linear increase in viscosity with concentration a-as seen in wulan gum (Lai et al. 2020). However, this linear relationship is questioned by findings from Olabode et al. (2023), where rheological experiments on Guar gum indicated that increases in polymer concentration enhance molecular interactions, leading to a viscosity increase from 900 cp. at 0.1 wt% to 1500 cp. at 1 wt% which is not linear. This study reflects more on what is depicted by *Beta vulgaris*. The observed variability in viscosity responses between natural polymers is attributed to differences in molecular weight and structural characteristics. Natural polymers derived from plants typically exhibit varying concentrations of the same compounds. For instance, *Beta vulgaris* contains bioactive compounds such as pectins, phenolics, and betalains, and their bioactivity is influenced

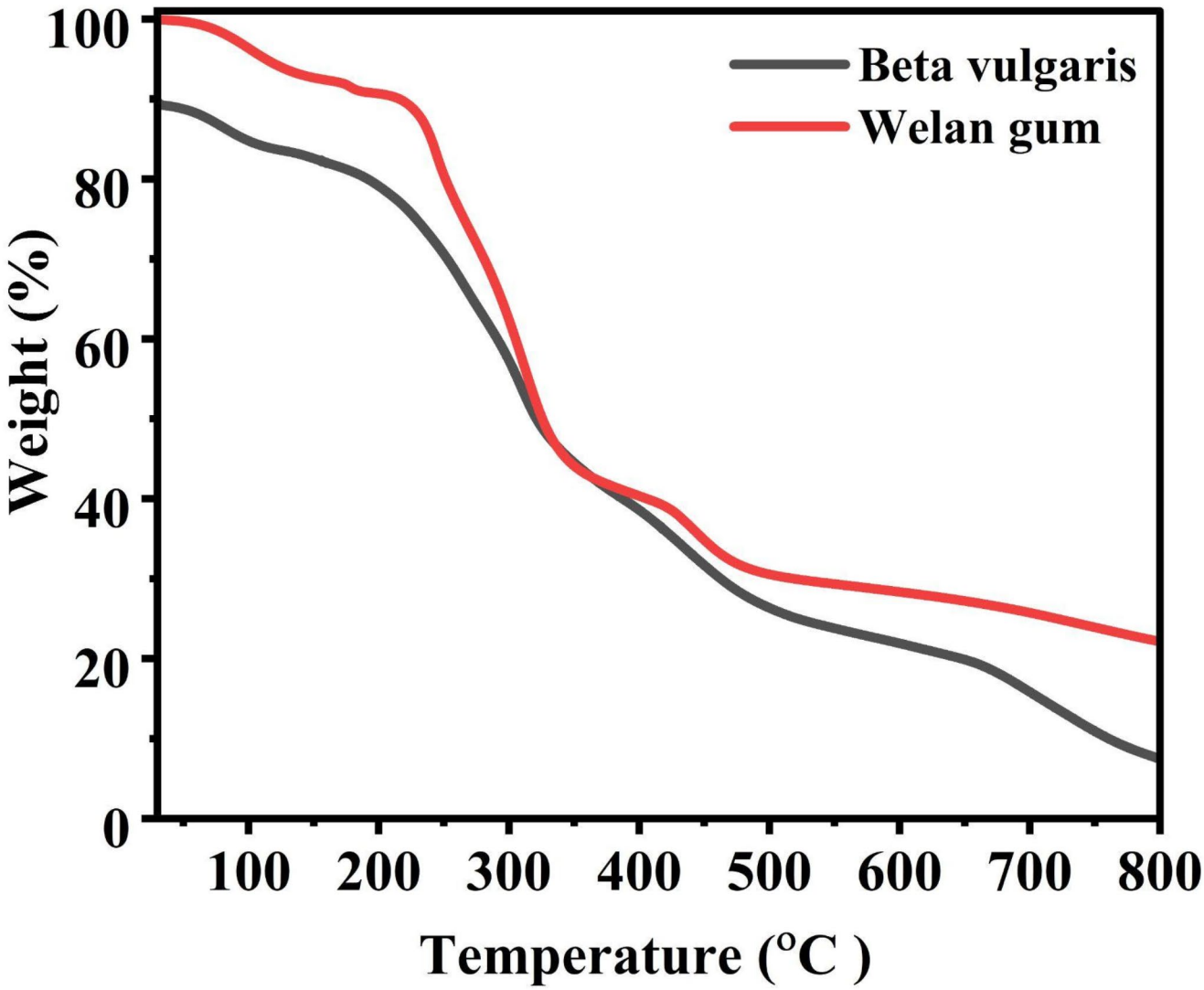



**Fig. 5** TGA of *Beta vulgaris* and Welan gum

by the plant's growth location and environmental factors including soil composition, climate, and farming practices (Carrillo et al. 2019). These investigations jointly assert the direct proportionality of polymer concentration to viscosity.

## Temperature effect on rheology

The effect of temperature was investigated by measuring viscosity from 25 to 55 °C to mimic Kazakhstan reservoir conditions. Both polymers, *Beta vulgaris* and Welan gum, were heated at different temperatures and analyzed at optimum concentrations of 10 wt% and 0.1 wt%, respectively. Figure 7a and b show the effect of temperature on the rheology of *Beta vulgaris* and Welan gum.

Figure 7a shows that *Beta vulgaris* viscosity decreases with the increase in temperature from 25 to 55 °C. Viscosity drops dramatically after increasing the temperature, which states that *Beta vulgaris* is not tolerant to high temperatures. From Fig. 6a, after increasing temperature to 30 °C viscosity has dropped from 10 cp. to 2 cp. at reservoir conditions. Overall viscosity drop was more than 80% at reservoir conditions.

This behavior is explained by the increase in kinetic energy through heating sites. Temperature rise in molecules affects the mobility of the molecule and reduces intermolecular forces of the long chains, weakening them. As bonding ability decreases, polymer chains pass each other and become detached from elongated chains. This heating results in huge viscosity reductions for *Beta vulgaris*.

Results from the pure Welan gum analysis in Fig. 7b show a small reduction in viscosity after heating the Welan gum solution. This study shows the performance of Welan gum under high temperatures without *Beta vulgaris* addition. Figure 7b clearly shows that all trends of Welan gum at

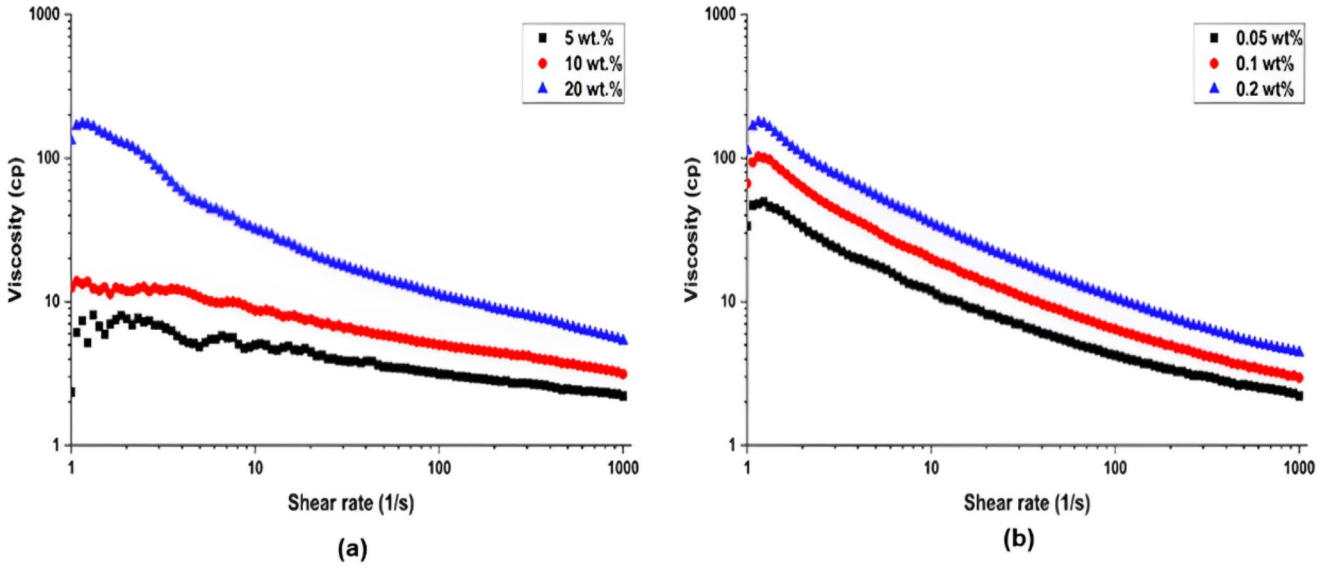



**Fig. 6** **a***Beta vulgaris* effect on rheology, **b** Welan gum effect on rheology

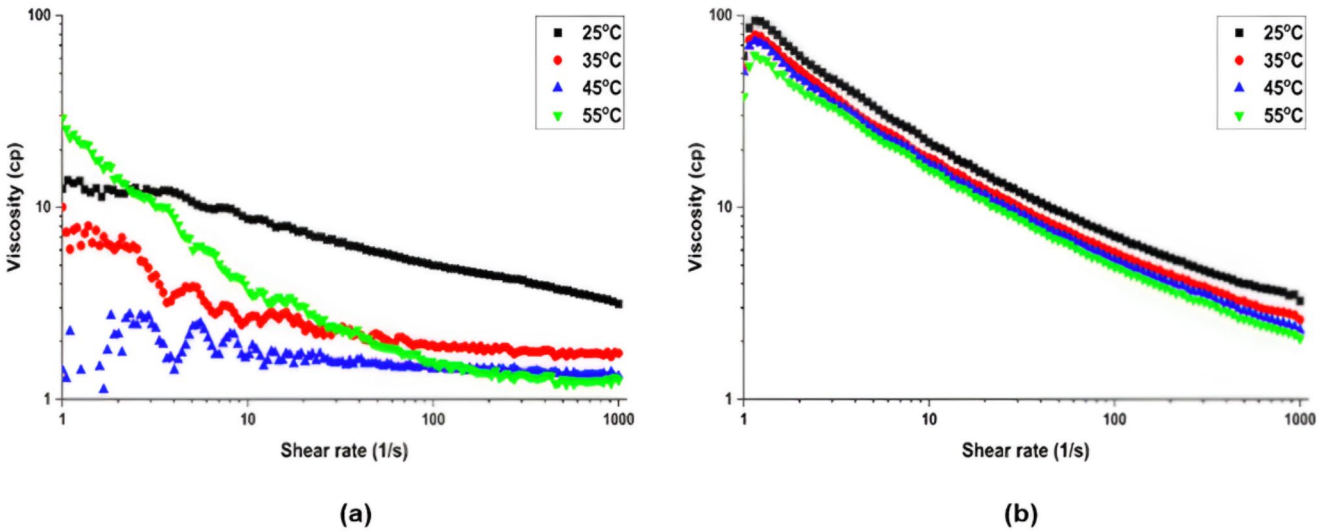



**Fig. 7** **a***Beta vulgaris* effect of temperature, **b** Welan gum effect of temperature

different temperatures are in one range, with a viscosity drop from 23 cp. to 18 cp. at reservoir conditions. Overall viscosity drop was around 20% at reservoir conditions, which indicates that Welan gum solution is tolerant to temperature rises in the reservoir. This in fact supports that the Welan gum solution could be benefitial as an additive to provide temperature resistance. The molecular structure of Welan gum could be the reason for the relatively great tolerance to temperature changes.

Despite welan temperature resistance, every polymer is expected to have viscosity reductions after heating. Another study also confirmed that most monosaccharides (biopolymers) show viscosity reductions with the increase in temperature at high polymer concentrations (Jouenne 2020). The employed polymer in this study confirms the natural polymer tolerance to temperature (Jouenne 2020). It is worth noting that synthetic polymers usually have higher viscosity drops at harsh reservoir conditions (Al-Shakry et al. 2018; Zhu et al. 2019). Previous studies reported designed polymer such as Floopam 3630 S showed that at 60 °C the viscosity is less as 10 cp. (Navaie et al. 2022).

## Salinity effect under reservoir conditions

The effect of seawater salinity as a main reservoir parameter is considered along with temperature to mimic harsh offshore field conditions. *Beta vulgaris* and Welan gum solutions were dissolved in 3.5 wt% NaCl solution and analyzed

through the rheometer. The study of salinity is motivated by the anticipated loss of the polymer's rheological properties when exposed to additional ions.

Figure 8a and b show rheology results for *Beta vulgaris* and Welan gum.As seen in Fig. 8a the presence of additional ions negatively impacts the viscosity of *Beta vulgaris*. Despite this decrease in viscosity, *Beta vulgaris* shows great salinity tolerance. After increasing salinity from DIW to 3.5 wt%, viscosity decrease was less than 30% from the original at shear rates of 10 $s^{-1}$. This viscosity slightly decreases, stating that *Beta vulgaris* has nonpolar functional groups. However, the effect of an increase in temperature and salinity destroys polymer molecules. The case of *Beta vulgaris* is viscosity reduction is more linked to the temperature tolerance rather that the salinity tolerance. Figure 8b shows that the Welan gum polymer loses all rheological properties after increasing salinity to 3.5 wt%. Results at ambient conditions (25 °C temperature) show that viscosity values range from 1 to 3 cp. The loss of rheological properties after increasing salinity is explained by possible breakage of hydrogen bonding connecting monomer molecules. Hydrogen bonds, typical bonding for monosaccharides, are highly vulnerable to positive sodium ions. A previous investigation by Khutoryanskiy et al. (2004) examined the impact of inorganic salts, such as NaCl, on hydrogen bonding in interpolymer complexes. Their findings revealed that as salt concentration rises, sodium ions cause partial dissociation of the polyacid's carboxylic groups, thereby reducing hydrogen bonding capacity. An increase in temperature was not even considered, as viscosity values are very low at every temperature, which is close to the water viscosity of 0.5 cp.

As it can be seen that for both polymers the salinity has sever adverse effect on the viscoisity. This generally could be explained by the coiling of long polymer molecules into large rings of colloids. Coiling of polymers into these rings reduces intermolecular contact of polymer chains and viscosity decreases approaching water viscosity. The coiling of polymers is explained by changing the polarity of polymer tails in the presence of additional cations and anions reaching the polar system. However, biopolymers are believed to be resistant to saline environments in nature. The main distinction is in functional groups and the low polarity of molecules, which do not form ionic bonds within molecules (Ciferri 2010; Gao 2015a, b). The interaction between ions and natural polymers is critical aspect to study thorugh the analysis of zeta potential (electrokinetic potential in colloidal systems). According to Wiśniewska et al. (2014), the primary mechanisms by which ions affect zeta potential is through the displacement of counter-ions in the electrical double layer surrounding the polymer. However, for the critical analysis laboratory experiments are needed.

## Progression in composite (blend of two natural polymers)

Employing the rheological data for *Beta vulgaris* and Welan gum, a composite material was engineered by blending 10 wt% of *Beta vulgaris* with 0.1 wt% Welan gum. The objective was to develop a composite that combines the salinity resistance of *Beta vulgaris* with the thermal stability of Welan gum, benefiting from the strengths of both polymers for enhanced performance. The results shown in Fig. 9 proved that the composite material is highly tolerant

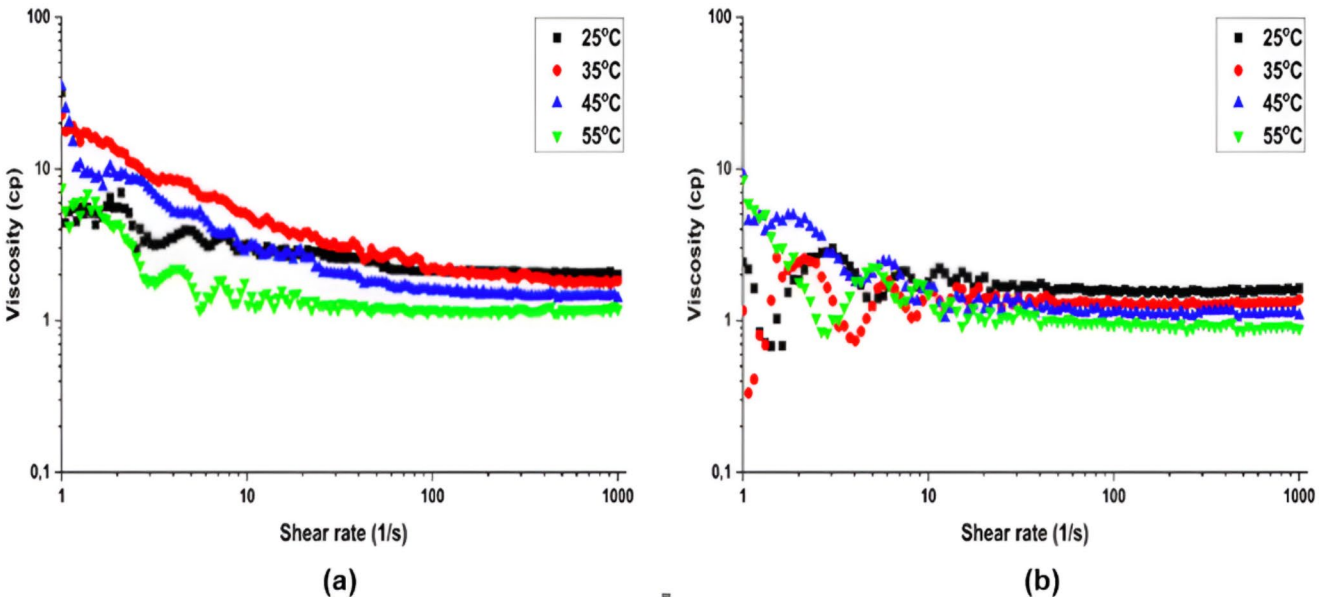



**Fig. 8** **a***Beta vulgaris* rheology at 3.5 wt% NaCl, **b** Welan gum rheology at 3.5 wt% NaCl

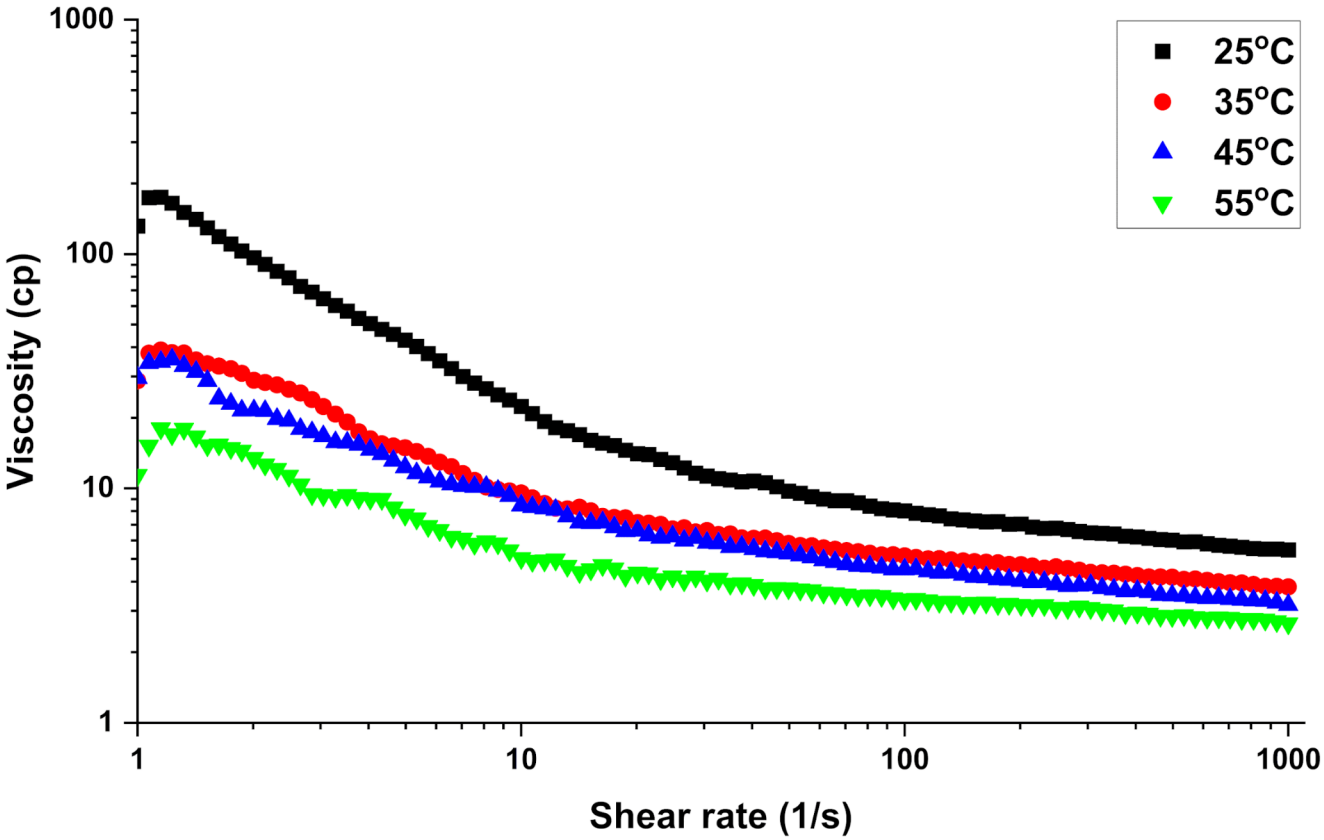



**Fig. 9** Composite polymer rheology under seawater salinity (3.5 wt%) and temperature

to salinity change, as viscosity values are accurate and identical to the original study in DIW. By analysing the temperature effect it also confirmed that the composite is temperature tolerant at high salinity. However, a notable deviation in the viscosity trend was observed at a shear rate of 350 $s^{-1}$, designated as region II in the plot, which was absent in previous studies. This new region is attributed to the unique composition and new functional groups formed in the composite.

The enhancement of rheological properties after mixing two different polysacchride polymers is attributed to several factors, including the structure of the polymers, their interaction, and the conditions under which they are mixed. For instance, the beta linkage between glucopyranosyl molecules encourages close packing and intermolecular hydrogen bonding, increasing rigidity.

In the given case, the study proposes several mechanisms of interaction between *Beta vulgaris* and Welan gum. All the reactions could be inferred from polysaccharides (Welan gum) and monosaccharides (*Beta vulgaris*) main character. The interaction can be by forming chemical links or physical interaction like polymer entalgments (Ahmed 2015). As seen earlier *Beta vulgaris* has Carboxyl groups which can allow–COOH of *Beta vulgaris* to form hydrogen bonds with the hydroxyl (–OH) groups of Welan gum. Also both polymers has hydroxyl group which forms stronger hydrogen bond in the water. This supports the chemical link between the polymer chains. For the physical entalgment it could occur since both polymers are prepared by heating which will make the welan gum -long chains- form physical knots to shorter chains in *Beta vulgaris* and form a stable network and restricted movement (Yang and Yang 2020). Welan gum morphology exhibited more uniform and defined rod-like structures which mirror compact characteristics as could be utilized as good candidate for physical interaction. Previous work claimed that increased temperature breaks high molecular weight polysaccharides into lower molecular weight forms by weakening hydrogen bonding(Lu et al. 2018). This phenomenon explains why temperature can influence the degradation and modification of polysaccharides, potentially reducing their rheological properties. However, the chemical bond between the molecules can over come this kientetic effect since the temperature is only limited to 55 °C. Evidently the improvement aids the applicability of the composite in offshore Kazakhastan.

## Shear thinning model

From Fig. 10, it can be seen that viscosity drops with the increase in shear rate. A decreasing trend with a shear rate increase is observed for all concentrations, and the viscosity drop is consistent. Viscosity reduction with the increase in shear rate is known as shear thinning fluid behavior. The nature of polymer molecules and the alignment of long polymer chains explain this behavior. In the case of natural polymers, long polymer chains align in the flow direction at high shear rates, consequently decreasing viscosity. Another reason is the nature of natural polymer molecules that might experience a decrease in the volume of polymer molecules at higher shear rates and a reduction in intermolecular forces (Abbas et al. 2022, 2024; Mazhit et al. 2023; Jalalvandi and Shavandi 2019; Nair and Choudhury 2020).

Polymers with shear thinning behavior are the main candidates for chemical EOR applications. Shear shinning polymers are easily injected into the wellbore at the lowest viscosity. According to Abbas et al. (2023), moderate shear rates between 150 $s^{-1}$ and 300 $s^{-1}$ correspond to the shear rates exerted on the wellhead region. Moreover, shear-thinning polymers reach the maximum viscosity values at the shear rates 7 $s^{-1}$ and 10 $s^{-1}$, representing the porous media range (Abbas et al. 2023). Shear-thinning polymers have the lowest viscosity in the period of injection and the highest viscosity values in the reservoir. It should be noted that polymers exhibit different rheological properties in three shear rate regions (I, II, III).

Lower Newtonian polymer behavior is found in the first region (I), where shear rate changes do not affect polymer viscosity. The insufficient shear rate level explains how this affects the polymer viscosity. Region I is present at low shear rates between 0.001 and 0.1 $s^{-1}$ and cannot be seen in the current experiment range. Region II is the region of interest, as polymer chains experience stretching and inclination from their original structure at these shear rates. Elongation of polymer chains and structure destruction under high shear stress reduces polymer viscosity. Constant viscosity decrease due to increased shear rate is characterized by the power law model of Ostwald–de Waele. For EOR application, viscosity readings at shear rate values corresponding to porous media are used.

Upper Newtonian polymer behavior corresponds to the third region (III), where polymer molecules lose rheological properties and are unaffected by shear rate changes. At the highest rates, polymer molecules break and elongated chains split, losing viscosity values, at peak values, no chains are observed in the solution. Region III is found in *Welan gum*

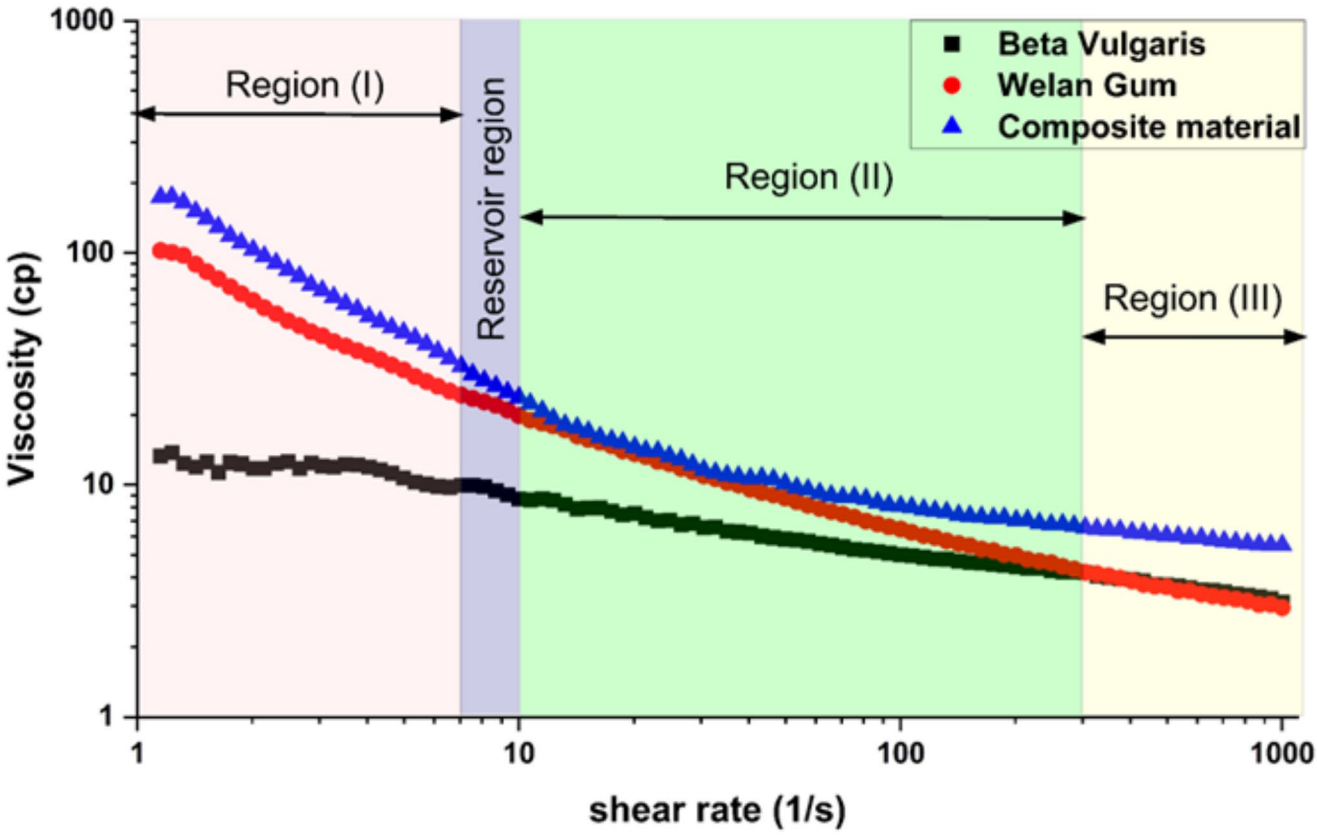



**Fig. 10** Concentration profile for polymers

**Table 3** Shear thinning model for *Beta vulgaris*

| Salinity (wt%) | Temperature (°C) | Concentration (wt%) | Flow behavior index (k) | Consistency index (*n*) | $R^2$ |
|---|---|---|---|---|---|
| 0 | 25 | 10 | 68.180 | 0.195 | 0.97 |
| | 35 | | 7.972 | 0.676 | 0.84 |
| | 45 | | 3.447 | 0.82 | 0.67 |
| | 55 | | 14.934 | 0.297 | 0.92 |
| 0.1 | 25 | 10 | 68.554 | 0.184 | 0.97 |
| | 35 | | 7.127 | 0.687 | 0.85 |
| | 45 | | 1.875 | 0.954 | 0.11 |
| | 55 | | 25.756 | 0.223 | 0.98 |
| 1 | 25 | 10 | 3.772 | 0.893 | 0.63 |
| | 35 | | 2.896 | 0.908 | 0.41 |
| | 45 | | 1.745 | 0.956 | 0.10 |
| | 55 | | 9.695 | 0.305 | 0.80 |
| 3.5 | 25 | 10 | 6.495 | 0.744 | 0.28 |
| | 35 | | 18.778 | 0.473 | 0.96 |
| | 45 | | 17.318 | 0.240 | 0.76 |
| | 55 | | 5.219 | 0.573 | 0.70 |

**Table 4** Shear thinning model for Welan gum

| Salinity (wt%) | Temperature (°C) | Concentration (wt%) | Flow behavior index (k) | Consistency index (*n*) | $R^2$ |
|---|---|---|---|---|---|
| 0 | 25 | 0.1 | 92.488 | 0.405 | 0.97 |
| | 35 | | 77.912 | 0.392 | 0.97 |
| | 45 | | 72.219 | 0.396 | 0.98 |
| | 55 | | 59.749 | 0.447 | 0.97 |
| 0.1 | 25 | 0.1 | 11.556 | 0.760 | 0.97 |
| | 35 | | 10.840 | 0.727 | 0.98 |
| | 45 | | 8.279 | 0.768 | 0.93 |
| | 55 | | 5.157 | 0.837 | 0.66 |
| 1 | 25 | 0.1 | 3.383 | 0.910 | 0.44 |
| | 35 | | 2.553 | 0.933 | 0.18 |
| | 45 | | 2.799 | 0.878 | 0.60 |
| | 55 | | 1.211 | 1.010 | 0.02 |
| 3.5 | 25 | 0.1 | 1.914 | 0.967 | 0.14 |
| | 35 | | 1.500 | 0.974 | 0.03 |
| | 45 | | 5.153 | 0.599 | 0.74 |
| | 55 | | 4.077 | 0.577 | 0.53 |

**Table 5** Shear thinning model for composite solution

| Salinity (wt%) | Temperature (°C) | Concentration | Flow behavior index (k) | Consistency index (*n*) | $R^2$ |
|---|---|---|---|---|---|
| 3.5 | 25 | 10 wt% + 0.1 wt% | 175.984 | 0.157 | 0.98 |
| | 35 | | 39.148 | 0.483 | 0.95 |
| | 45 | | 32.817 | 0.483 | 0.95 |
| | 55 | | 16.115 | 0.618 | 0.9 |

solution at shear rates greater than 300 $s^{-1}$, viscosity values at these ranges approach water viscosity of 1 cp.

Tables 3 and 4, and 5 show shear thinning data for *Beta vulgaris*, Welan gum, and composite solution under reservoir temperature and seawater salinity, respectively.

From Tables 3 and 4, the decreasing trend in flow behavior factor (k) and increasing trend in consistency factor is observed after the temperature rises from 25 to 55 °C. Generally, k values characterize the flow resistance of a fluid under low shear rates; a decrease in k values consequently states a loss of viscosity at low shear rates. This behavior confirms the original statement about the effect of temperature on polymer viscosity. In the case of the consistency index, n values constantly increase with temperature rise and approach value of 1. As the n value of 1 corresponds to Newtonian fluid behavior, these results confirm the loss of shear-thinning rheological properties of the polymer under high temperatures. An additional increase in salinity affects both flow behavior and consistency indexes similarly. This states that the simultaneous effect of temperature and salinity worsens original rheological properties more than the temperature effect alone, confirming the low resistance of *Beta vulgaris* and Welan gum to temperature and salinity. It should be noted that measurements and power law correlations were not highly accurate due to the low viscosity of materials. This is seen from $R^2$ values for both polymers in the 50–90% range. Conversely, Table 5 shows highly accurate results of data measurements with an average error of 95%. Given composite polymer at high salinity conditions (3.5 wt%), it has high flow behavior and low consistency index values. This confirms the great tolerance of composite material to high salinity environments and the avoidance of polymer breakage and coiling. Although increased temperature decreases the flow behavior index and increases the consistency factor, shear thinning behavior is still present in the fluid. This is confirmed by the consistency index, which reaches the peak value of 0.618 in a range of non-Newtonian behavior. Moreover, the flow behavior index decrease is lower than in *Beta vulgaris* and Welan gum material. Overall, composite polymer is superior to *Beta vulgaris* and Welan gum material at high temperature and salinity conditions.

## EOR displacement study

Indiana limestone core was used in the main core flooding experiment. Measured porosity and permeability values are 18.5% and 180 mD, respectively. The composite material was injected into the decane-saturated core after main saline waterflooding and results of the core flooding experiment are shown in Table 6.

**Table 6** Results of core flooding experiment

| Parameters | Core 1 |
|---|---|
| Composite material viscosity at 25 C (cp.) | 22.4 |
| *Beta vulgaris* concentration (wt%) | 10 |
| Welan gum concentration (wt%) | 0.1 |
| Salinity (wt%) | 3.5 |
| Oil relative permeability (ko) | 127 |
| PVs of water breakthrough | 1 |
| Initial water saturation | 25.8% |
| Recovery factor after water flooding | 48% |
| Incremental oil recovery after polymer flooding | 11% |
| Incremental oil recovery after 2 cycly water flooding | 5% |
| Final recovery factor | 64% |
| Final oil saturation | 26.4% |

From Table 6, 48% of the original oil in place was recovered through waterflooding, Fig. 11 shows the general trend of oil recovery vs. pore volume injected in red and blue lines for polymer and waterflooding, respectively. The first recovered oil droplet was observed after the injection of 1 PV of saline water. After 5 PV of saline water injection, 1 PV of composite material was injected with an estimated viscosity of 22.4 cp. The main flush injection resulted in an additional 11% of oil recovered from 1 PV of polymer solution injected. Further injection of saline water as a post-flush resulted in an additional 5% of oil recovered. Generally, composite injection increased recoverable oil to 16%, which is considered a successful result.

Comparing the results of the following work with the existing studies on the application of Welan gum in enhanced oil recovery as a viscosifying agent, profound similarities in the properties were identified. Gao and Technology (2015), studied the effect of salinity on Welan gum at different concentrations of NaCl solution. Results have shown that the viscosity drop after salinity rise from 10 to 100 g $L^{-1}$ of NaCl resulted in only 8% of viscosity drop of Welan gum. Another study by Xu et at confirmed great displacing efficiency of Welan gum on heavy oil flooding. Injection of highly viscous Welan gum resulted in 35% of additional oil recovery.

Results from Fig. 11 show that injection of composite polymer solution significantly increases pressure drop from the inlet to the outlet of the core. This pressure rise was observed throughtout polymer composite material injection period after 5 PV of water. Pressure increase in the core is explained by the higher resistance of injected fluid to flow in the porous media. As the flow rate was held constant during the data recording, the waterflooding pressure drop was around 20 psi. After the injection of 1 PV of composite

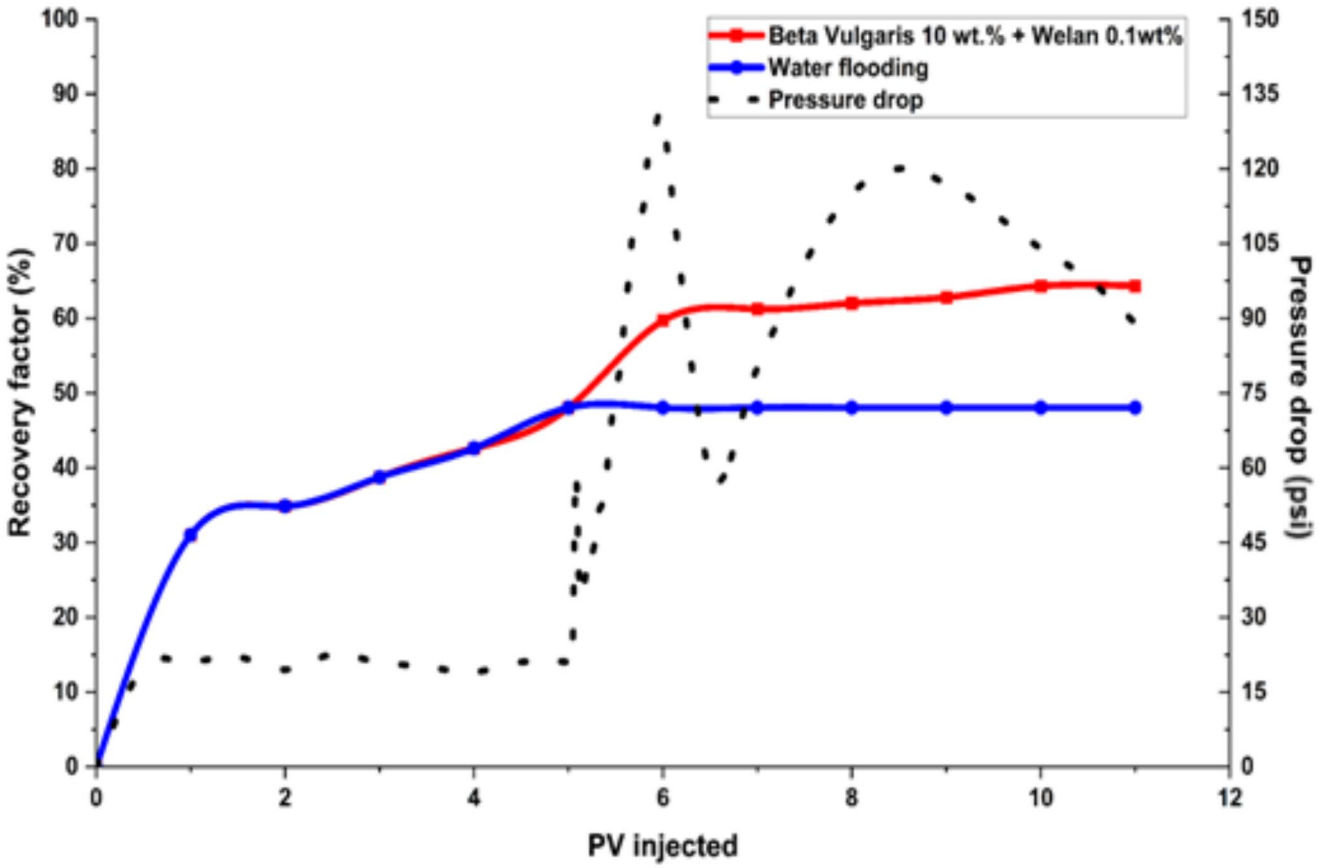



**Fig. 11** Recovery factor and pressure drop profiles from core flooding

material, the pressure drop reached the maximum value of 135 psi across the core. This observation confirms that fluid flow through porous media is restricted and injected fluid has high viscosity. After the injection of water as a post-flush, the pressure drop reaches a peak of 80 psi, and decreases to the second maximum value, confirming that polymer molecules were flooded from a core. This variation of pressure drop is explained by the change of mobility ratio in the core system and flow restriction. As for initial water flooding into oil saturated core small pressure drop is expected, while in the polymer composite injection high pressure drop is explained by the decrease in mobility ratio due to high viscosity of the fluid. For the final post water injection, remaining polymer solution was pushed by the post-flush water resulting in higher pressure drop compared to initial water injection. In statistical terms, the addition of polymers to the waterflood enhances the fractional flow of oil (Fo) from 0.45 to 0.74 with natural polymers, and from 0.45 to 0.95 with composite polymers, signifying a good increase in oil recovery efficiency up to 26%. This is attributed to the increased viscosity of water. Overall, natural polymers can increase oil fractional flow to around 60%, and 26% of incremental oil recovery with combination of these polymers in a composite material.

Discussions on polymers always highlight the direct relationship between a flood's recovery efficiency and mobility ratio through the mechanisms of decreasing water relative permeability ($kw$) or increasing water viscosity ($\mu w$). This improvement in mobility ratio is more pronounced when the mobile oil saturation is relatively high. For the current study, the mobility ratio during waterflooding is 1.3. It can be described as good mobility. Yet, the enhancement by the polymer and composite is also remarkable. The mobility ratio became 1.04 and 0.04 for the natural polymer and the composites, respectively. By looking at the main two concepts, it can be predicted that polymer flooding brings faster oil movement due to better fractional flow and the ability to sweep the core area, as indicated by the improved mobility ratio. Despite the displacement, it proves that limestone pore size distribution is heterogeneous, including intergranular and intragranular micropores. The selected polymer and composite can be advantageous if considered their expected ability to work as a fluid diversion.

## Conclusions

- This study introduced a novel approach by utilizing natural polymers, specifically *Beta vulgaris* and Welan gum, for Enhanced Oil Recovery (EOR), particularly in offshore applications.
- *Beta vulgaris* exhibited significant salinity tolerance but showed reduced viscosity at high temperatures. Welan gum, on the other hand, maintained viscosity stability at elevated temperatures but was weakened by high salinity.
- The composite polymer blend demonstrated enhanced thermal and salinity tolerance, resulting in a viscosity range of 10 to 30 cP, suitable for offshore EOR applications in varying conditions.
- The crystalline structure of *Beta vulgaris* and the amorphous structure of Welan gum were confirmed by X-ray diffraction (XRD), while thermogravimetric analysis (TGA) highlighted their comparable thermal resistances.
- Core flooding experiments using the composite polymer in oil-wet limestone cores yielded a 16% increase in oil recovery, showcasing the potential of these natural polymers for improving oil recovery in harsh offshore environments.
- The innovative use of a composite blend of natural polymers provides an environmentally friendly, cost-effective alternative for polymer flooding in the petroleum industry.

**Acknowledgements** The authors would like to thank Aizahn Rakhimnova for her support during the characterization process. The authors would like to thank Dr. Changhong Gao for his insight on welan gum polymer.

**Author contributions** Galymzhan Serikov: Experimental, Investigation, Original Draft. Yermukhan Zhuniskenov: Methodology, Investigation, Experimental. Azza Hashim Abbas: Conceptualization, Methodology, Investigation, Validation, Supervision. Peyman Pourfashary: Supervision, Review, Editing.

**Funding** The authors would like to thank Nazarbayev University for supporting this research through the NU Faculty Development Competitive Research Grants Program (Grant numbers: 20122022FD4137 (AHA).

## Declarations

**Conflict of interest** The authors declare that they have no known competing financial interests or personal relationships that could have appeared to influence the work reported in this paper.

**Open Access** This article is licensed under a Creative Commons Attribution 4.0 International License, which permits use, sharing, adaptation, distribution and reproduction in any medium or format, as long as you give appropriate credit to the original author(s) and the source, provide a link to the Creative Commons licence, and indicate if changes were made. The images or other third party material in this article are included in the article's Creative Commons licence, unless indicated otherwise in a credit line to the material. If material is not included in the article's Creative Commons licence and your intended use is not permitted by statutory regulation or exceeds the permitted use, you will need to obtain permission directly from the copyright

holder. To view a copy of this licence, visit http://creativecommons.org/licenses/by/4.0/.

## References


Abbas AH, Ajunwa OM, Mazhit B, Martyushev DA, Bou-Hamdan KF, Alsaheb RAA (2022) Evaluation of OKRA (Abelmoschus esculentus) macromolecular solution for enhanced oil recovery in Kazakhstan carbonate reservoir. Energies 15:6827

Abbas AH, Serikov G, Zhuniskenov Y, Eghtesadi N, Bou-Hamdan KF, Pham TT (2023) Investigation of natural mucilage for enhanced oil recovery: the potential of corchorus olitorius hydrocolloid. ACS Omega 8:29693–29703

Abbas AH, Keldibayev N, Pourafshary P, Zhuniskenov Y, Serikov G (2024) Numerical simulation of flaxseed gum potential in improving oil recovery: focus on offshore Kazakhstan. Offshore Technology Conference Asia, D021S014R005

Adenutsi CD, Turkson JN, Wang L, Zhao G, Zhang T, Quaye JA, Erzuah S, Sokama-Neuyam YA (2023) Review on potential application of saponin-based natural surfactants for green chemical enhanced oil recovery: perspectives and progresses. Energy Fuels

Agi A, Junin R, Gbonhinbor J, Onyekonwu M (2018) Natural polymer flow behaviour in porous media for enhanced oil recovery applications: a review. J Pet Explor Prod Technol 8:1349–1362

Agi A, Junin R, Arsad A, Abbas A, Gbadamosi A, Azli NB, Oseh J (2019) Synergy of the flow behaviour and disperse phase of cellulose nanoparticles in enhancing oil recovery at reservoir condition. PLoS One 14:e0220778

Ahmed EM (2015) Hydrogel: preparation, characterization, and applications: a review. J Adv Res 6:105–121

Al-Shakry B, Shiran BS, Skauge T, Skauge A (2018) Enhanced oil recovery by polymer flooding: optimizing polymer injectivity. SPE Kingdom of Saudi Arabia Annual Technical Symposium and Exhibition, Society of Petroleum Engineers

Bai B, Zhou J, Yin M (2015) A comprehensive review of polyacrylamide polymer gels for conformance control. Pet Explor Dev 42:525–532

Bhut PR, Pal N, Mandal A (2019) Characterization of hydrophobically modified polyacrylamide in mixed polymer-gemini surfactant systems for enhanced oil recovery application. ACS Omega 4:20164–20177

Brezhneva TA, Nikolaevskii VA, Selemenev VF, Slivkin AI, Muad AA, Khind T, Safonova EF (2001) Isolation of saponins from Sugar Beet roots and preliminary characterization of their Adaptogen Properties. Pharm Chem J 35:159–161

Cai Z, Guo Y, Ma A, Zhang H (2024) NMR analysis of the side-group substituents in welan gum in comparison to gellan gum. Int J Biol Macromol 254:127847

Carrillo C, Wilches-Pérez D, Hallmann E, Kazimierczak R, Rembiałkowska E (2019) Organic versus conventional beetroot. Bioactive compounds and antioxidant properties. LWT 116:108552

Ciferri A (2010) Ionic mixed interactions in macromolecules. Chem Eur J 16:10930–10945

Druetta P, Picchioni F (2019) Polymer and nanoparticles flooding as a new method for enhanced oil recovery. J Pet Sci Eng 177:479–495

Druetta P, Raffa P, Picchioni F (2019) Chemical enhanced oil recovery and the role of chemical product design. Appl Energy 252:113480

Ezeh O, Ikiensikimama SS, Akaranta O (2021) Critical review of polymer flooding in daqing field and pelican field: case studies of the world's largest polymer flooding in light and heavy oil reservoirs, respectively. J Eng Res Rep 21:25–40

Ferreira VH, Moreno RB (2020) Experimental evaluation of low concentration scleroglucan biopolymer solution for enhanced oil recovery in carbonate. Oil Gas Sci Technol 75:61

Fredi G, Dorigato A (2023) Compatibilization of biopolymer blends: a review. Adv Ind Eng Polym Res 7:373–404

Fu L, Jiang L, Liao K, An J, Huang W, Sun X, Li T, He Y (2021) Adsorption behavior of welan gum on quartz sand in reservoir. J Pet Sci Eng 205:108850

Gao C (2015a) Potential of Welan Gum as mud thickener. J Pet Explor Prod Technol 5:109–112

Gao C (2015b) Potential of Welan gum to enhance oil recovery. J Pet Explor Prod Technol 5:197–200

Gao C (2016) Potential applications of Welan gum in upstream petroleum industry. Int J Oil Gas Coal Eng 4:16

Gao Z-J, Han X-H, Xiao X-G (2009) Purification and characterisation of polyphenol oxidase from red Swiss chard (*Beta vulgaris* subspecies cicla) leaves. Food Chem 117:342–348

Gbadamosi A, Patil S, Kamal MS, Adewunmi AA, Yusuff AS, Agi A, Oseh JJP (2022a) Application of polymers for chemical enhanced oil recovery: a review. Polymers 14:1433

Gbadamosi A, Zhou X, Murtaza M, Kamal MS, Patil S, Al Shehri D, Barri AJP (2022b) Experimental study on the application of cellulosic biopolymer for enhanced oil recovery in carbonate cores under harsh conditions. Polymers 14:4621

Han D-K, Yang C-Z, Zhang Z-Q, Lou Z-H, Chang Y-I (1999) Recent development of enhanced oil recovery in China. J Pet Sci Eng 22:181–188

Jalalvandi E, Shavandi A (2019) Shear thinning/self-healing hydrogel based on natural polymers with secondary photocrosslinking for biomedical applications. J Mech Behav Biomed Mater 90:191–201

Jouenne S (2020) Polymer flooding in high temperature, high salinity conditions: selection of polymer type and polymer chemistry, thermal stability. J Pet Sci Eng 195:107545

Kale R, Sawate A, Kshirsagar R, Patil B, Mane R (2018) Studies on evaluation of physical and chemical composition of beetroot (*Beta vulgaris* L). Int J Chem Stud 6:2977–2979

Khan I, Mansha M, Jafar Mazumder MA (2019) Polymer blends. In: Mazumder JAFAR, Sheardown MA, H., Al-Ahmed A (eds) Functional polymers. Springer International Publishing, Cham pp 513–549

Khutoryanskiy VV, Mun GA, Nurkeeva ZS, Dubolazov AV (2004) pH and salt effects on interpolymer complexation via hydrogen bonding in aqueous solutions. Polym Int 53:1382–1387

Klecker C, Nair LS (2017) Matrix chemistry controlling stem cell behavior. *Biol Eng Stem Cell Niches.* Elsevier

Kong L, Yu L, Feng T, Yin X, Liu T, Dong L (2015) Physicochemical characterization of the polysaccharide from Bletilla striata: effect of drying method. Carbohydr Polym 125:1–8

Lai NJ, Wen YP, Yang ZD, Chen JL, Zhao XB, Wang DD, He W, Chen YM (2020) Polymer flooding in high-temperature and high-salinity heterogeneous reservoir by using diutan gum. J Pet Sci Eng 188:106902

Li Q, Pu W, Wei B, Jin F, Li K (2017) Static adsorption and dynamic retention of an anti-salinity polymer in low permeability sandstone core. J Appl Polym Sci 134(8)

Lu X, Li N, Qiao X, Qiu Z, Liu P (2018) Effects of thermal treatment on polysaccharide degradation during black garlic processing. LWT 95:223–229

Mazhit B, Abbas AH, Pourafshary P (2024) Evaluation of Flaxseed Hydrocolloid's potential in improving oil recovery. J King Saud Univ Eng Sci 36:611–618

Musa TA, Ibrahim AF, Nasr-El-Din HA, Hassan A (2021) New insights into guar gum as environmentally friendly polymer for enhanced oil recovery in high-salinity and high-temperature sandstone reservoirs. J Pet Explor Prod 11:1905–1913

Mzoughi Z, Chahdoura H, Chakroun Y, Cámara M, Fernández-Ruiz V, Morales P, Mosbah H, Flamini G, Snoussi M, Majdoub H (2019) Wild edible Swiss chard leaves (*Beta vulgaris* L. var. cicla): Nutritional, phytochemical composition and biological activities. Food Res Int 119:612–621

Nair R, Choudhury AR (2020) Synthesis and rheological characterization of a novel shear thinning levan gellan hydrogel. Int J Biol Macromol 159:922–930

Navaie F, Esmaeilnezhad E, Choi H-J (2022) Effect of rheological properties of polymer solution on polymer flooding characteristics. Polymers 14:5555

Needham RB, Doe PH (1987) Polymer flooding review. J Pet Technol 39(1,503–1):507

Nowrouzi I, Mohammadi AH, Manshad AK (2023) A natural polymer extracted from Chia seeds for application in chemical enhanced oil recovery by taper polymer concentration (TPC) and alkali-polymer (AP) slug injection into sandstone oil reservoirs. Fuel 350:128738

Ojo Oladimeji V, Onyekonwu M, Ogolo N, Ubani C (2013) Effect of Viscosity of Alkaline/Surfactant/Polymer on Enhanced Oil Recovery in Heterogeneous Sands. SPE Nigeria Annual International Conference and Exhibition, SPE, SPE-167550-MS

Olabode O, Akinsanya O, Daramola O, Sowunmi A, Osakwe C, Benjamin S, Samuel I (2023) Effect of Salt concentration on oil recovery during polymer flooding: Simulation studies on Xanthan Gum and Gum Arabic. Polymer 15:4013

Pal N, Babu K, Mandal A (2016) Surface tension, dynamic light scattering and rheological studies of a new polymeric surfactant for application in enhanced oil recovery. J Pet Sci Eng 146:591–600

Pal N, Kumar N, Mandal A (2019) Stabilization of dispersed oil droplets in nanoemulsions by synergistic effects of the gemini surfactant, PHPA polymer, and silica nanoparticle. Langmuir 35:2655–2667

Pramadika H, Samsol S, Satiyawira B (2019) The effect of addition of polymer on viscosity as fluid of industrial oil and gas injection in EOR method. J Phys Conf Ser 1402:022053

Pu W, Shen C, Wei B, Yang Y, Li Y (2018) A comprehensive review of polysaccharide biopolymers for enhanced oil recovery (EOR) from flask to field. J Ind Eng Chem 61:1–11

Quiroga-Becerra H, Mejía-Miranda C, Laverde-Cataño D, Hernández-López M, Gómez-Sánchez M (2012) A kinetic study of esterification of naphthenic acids from a Colombian heavy crude oil. CT&F-Ciencia Tecnología Y Futuro 4:21–31

Sun L, Zhang Z, Leng K, Li B, Feng C, Huo X (2022) Can supramolecular polymers become another material choice for polymer flooding to enhance oil recovery? Polymers 14:4405

Wever D, Picchioni F, Broekhuis A (2011) Polymers for enhanced oil recovery: a paradigm for structure–property relationship in aqueous solution. Prog Polym Sci 36:1558–1628

Wiśniewska M, Urban T, Grządka E, Zarko VI, Gun'ko VM (2014) Comparison of adsorption affinity of polyacrylic acid for surfaces of mixed silica–alumina. Colloid Polym Sci 292:699–705

Yang D, Yang H (2020) The temperature dependent extraction of polysaccharides from eucheuma and the rheological synergistic effect in their mixtures with kappa carrageenan. LWT 129:109515

Zamani AM, Moslemi A, Hassani K (2023) Experimental investigation into effects of the natural polymer and nanoclay particles on the EOR performance of chemical flooding in carbonate reservoirs. Pet Sci 21:951–961

Zhao M, Hu Y, Yao H, Huang J, Li S, Xu H (2022) Sustainable production and characterization of medium-molecular weight welan gum produced by a Sphingomonas sp. RW. Carbohydr Polym 289:119431

Zhao M, Liu K, Meng X, Ma Z, Dai C (2024) Review on principles, influence and applications of nanomaterials in enhancing oil recovery. Fuel 371:131985

Zhu D, Hou J, Wei Q, Chen Y (2019) Development of a high-temperature-resistant polymer-gel system for conformance control in Jidong oil field. SPE Reserv Eval Eng 22:100–109

**Publisher's note** Springer Nature remains neutral with regard to jurisdictional claims in published maps and institutional affiliations.